Twenty-Seventh Symposium (International) on Combustion/The Combustion Institute, 1998/pp. 1737–1744

SOURCES OF UNBURNED CARBON IN THE FLY ASH PRODUCED FROM LOW-NO_x PULVERIZED COAL COMBUSTION

JOHN M. VERANTH,[1] DAVID W. PERSHING,[1] ADEL F. SAROFIM[1] AND JEFFREY E. SHIELD[2]

[1]*Department of Chemical and Fuels Engineering*
[2]*Department of Materials Science*
University of Utah
Salt Lake City, UT 84112-1109, USA

The unburned carbon in the fly ash produced from low-NO_x pulverized coal combustion is shown to consist of a mixture of soot and coal char. The soot was identified by the presence of chains or aggregates of 10–50-nm-diameter primary particles in electron microscope images of both laboratory samples and a sample of fly ash from a power plant operating low-NO_x burners. Laboratory samples showed increasing carbon content with decreasing nitrogen oxide (NO_x) concentration. The experiments included a high-NO_x base case and four low-NO_x cases consisting of (1) staged combustion with short (0.5 s) residence time, (2) staged combustion with long (1.5 s) residence time, (3) a low-NO_x burner with slow mixing, and (4) reburning using coal as the reburning fuel. Comparison of the base case that used premixed coal and air with the long-residence-time staged combustion case shows a decrease in the NO_x from over 900 ppm to below 200 ppm and an increase in the carbon in the ash from 4% to over 30%. The fly ash from staged combustion was a mixture of large soot aggregates, porous char, and spherical particles of mineral ash, whereas the ash from reburning lacked the large aggregates. For all laboratory conditions, the carbon content in the particle fraction with an aerodynamic diameter over 10 μm was higher than in the 1–2.5-μm-diameter fraction. Both soot aggregates and char contributed to the high carbon in the large particle fraction. The difference in carbon burnout between the two staging conditions was consistent with published soot oxidation rates. Both char burnout and soot formation need to be considered in studies of the carbon content of pulverized coal fly ash.

Introduction

The level of nitrogen oxides (NO_x) produced by pulverized coal combustion can be reduced by staged combustion, low NO_x burners, low excess air operation, and reburning [1]. Creation of oxygen-deficient furnace regions minimizes the conversion of fuel nitrogen to NO_x but also inhibits the oxidation of carbon species, resulting in a high carbon content in the fly ash [2,3]. Carbon in the fly ash is undesirable because the carbon represents wasted fuel and prevents using the ash for cement production. The mutagenicity of coal fly ash has been associated with the organic content [4–6].

When a pulverized coal particle is injected into a flame, it decomposes into char and volatiles, and the volatiles further decompose to produce soot that creates a luminous zone surrounding the source particles [7,8]. Char refers to porous, carbon-rich particles that remain in a solid or liquid phase, and soot refers to carbon-rich solid material produced from gas-phase precursors.

Soot formation in pulverized coal flames has been studied because it affects both nitrogen evolution [9] and radiative heat transfer. Most studies of residual carbon in coal fly ash, however, have focused on the unburned char [10–12]. Soot was assumed to make a negligible contribution to carbon in the ash because soot particles, although less reactive than char, are also orders of magnitude smaller [13]. The sooting tendency of coal varies with rank [7], and soot aggregates have been reported to form in the wake of coal particles burning in a laminar flow laboratory furnace [14,15]. At least one study [14] speculated that staged combustion would enhance the tendency to form large soot aggregates in full-scale furnaces.

Methods

Both laboratory-generated samples and a filter sample obtained from the stack of a coal-fired power plant were used in this study. The laboratory samples were produced in a 29-kW, down-fired, U-shaped furnace with an inside diameter of 0.16 m and an overall length of 7.3 m. Ports along the length of the furnace are available for injecting fuel or air and for extracting samples. The furnace has a Reynolds number, based on furnace diameter, of 1000–2000, depending on stoichiometric ratio and temperature. A high-volatile, bituminous-*b* Utah coal, from the Wasatch Plateau field, was pulverized to 70% less

TABLE 1
Nominal combustion conditions used in this study

Condition Description		BASE Base Case	STG@1.5S Staging—Long Time	STG@0.5S Staging—Short Time	AXIAL Long Axial Flame	REBURN Coal Reburning
Burner configuration		premix	premix	premix	diffusion	premix
Thermal input, coal	KW	29.3	29.3	29.3	29.3	6.4
Thermal input, natural gas	KW	none	none	none	0.99	29.3
Distance to air staging port	m	[a]	3.17	1.36	[a]	[a]
Time to air staging port	s		1.5	0.5		
Distance to reburning port	m	[a]	[a]	[a]	[a]	2.89
Time to reburning fuel port	s					1.1
Distance to burnout air port	m	[a]	[a]	[a]	[a]	3.73
Time to burnout air port	s					1.4
Distance to exit sampling port	m	6.17	6.17	6.17	6.17	6.17
Time to exit sampling port	s	2.78	3.12	2.90	2.82	2.35
Target reducing zone S.R.[b]		[a]	0.85	0.85	variable	0.85
Target exit S.R.[b]		1.15	1.15	1.15	1.15	1.15
Exit oxygen concentration	%	2.87 ± 0.41	2.89 ± 0.38	2.78 ± 0.15	3.15 ± 0.5	2.78 ± 0.12
Exit NO_x concentration	ppm	947 ± 32	171 ± 17	465 ± 29	456 ± 56	242 ± 7
Number of runs for gas composition		14	17	16	8	6
Temperature 2 m from burner	K	1382 ± 17	1322 ± 4	1355 ± 26	1389 ± 9	1382 ± 38
Temperature at exit port	K	855 ± 19	818 ± 7	845 ± 12	803 ± 16	902 ± 23

[a] n/a: not applicable.
[b] S.R.: stoichiometric ratio.
[c] Measured data are the mean ± standard deviation for the available furnace sampling runs.

than 200 mesh. The coal heating value was 29 MJ/kg, and the ASTM volatiles were 40% on a dry basis with 9% ash. The furnace, coal burners, gas analysis instruments, and coal analysis are described elsewhere [16,17].

The test conditions are summarized in Table 1. The base case (abbreviated BASE) used a premixed burner in which the coal and combustion air passed through a water-cooled grid into the furnace. This simulates the rapid fuel and air mixing that occurs in older boiler designs. Two experimental conditions used this same premixed burner in conjunction with staged combustion. The coal devolatilization and the initial char oxidation took place at an overall stoichiometric ratio of 0.85, then burnout air was added that brought the stoichiometric ratio to 1.15. The staging air was added at ports that gave residence times in the reducing zone of approximately 0.5 s for condition STG@0.5S and 1.5 s for condition STG@1.5S, respectively. The low-NO_x burner condition (abbreviated AXIAL) used a long axial flame produced by concentric injection of natural gas, coal plus primary air, stabilization natural gas, and secondary air, which created reducing conditions in the core of the flame. For condition REBURN, an ammonia-spiked natural gas flame was used to simulate the combustion products of a low-NO_x coal burner. Pulverized coal followed by burnout air were injected downstream to create a short reducing zone. The stoichiometric ratio was calculated as the measured moles of oxygen supplied divided by the calculated oxygen for complete combustion based on the coal analysis.

The exit temperature and oxygen and NO_x (sum of nitrogen oxide and nitrogen dioxide) concentrations were continuously logged during the experiments. The furnace temperature was measured using a ceramic-sheathed type B thermocouple that was able to operate for extended periods, even with the high ash loading produced in the core of a pulverized coal flame. A previous study documented the difference between the type B thermocouple reading and suction pyrometer readings [16].

A water-cooled probe was used to collect the furnace gas and particles. Preliminary experiments indicated that the selected procedures produced acceptable samples of the particles smaller than 10-μm aerodynamic diameter [17]. Larger particles settle along the horizontal portion of the furnace and cannot be collected quantitatively. Rapid dilution at the probe tip was not used because the transport time inside the probe was small compared to the time from the burner to the sampling port. Either 90-mm

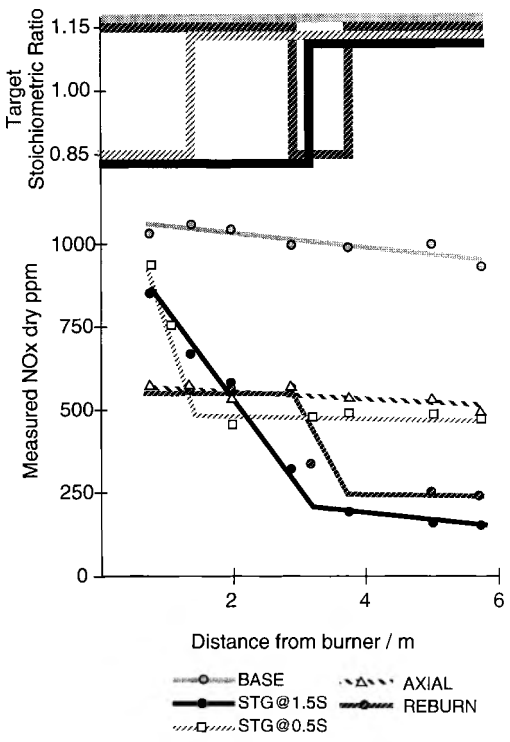

FIG. 1. Stoichiometric ratio and NO_x versus furnace location. The upper portion shows the target overall S.R. with step changes at the combustion ports. NO_x data are the average of three measurements each for the base case and the four experimental conditions. NO_x values between measurements are interpolated assuming that the slope changes at the injection ports.

glass fiber (Whatman 934-AH) or 0.22-μm polyvinyldiene fluoride membrane (Millipore GVHP) filters in a preheated holder were used to collect bulk samples. Both the filter deposit and the material washed from the probe were analyzed.

An Andersen 8-stage 1-acfm cascade impactor and preseparator were used with methods that were originally developed to produce large samples of oil-free particles for toxicology studies [18]. A fraction enriched in particles larger than 10-μm aerodynamic diameter was collected in the preseparator. The deposits collected on impactor stages 1, 2, and 3 were combined to make a sample enriched in particles between 2.5 and 10 μm. Stage 5 produced a sample enriched in particles between 1 and 2.5 μm. Stage 7 plus the final filter were combined to produce a sample of submicron particles. Oiled substrates were used on impactor stages 1, 4, and 6 to provide a separation.

The power plant sample came from a facility burning an eastern United States bituminous coal. The plant reported having a "dark stack" when operating the burners in a low-NO_x mode with overfire air. A sample of loose, black particles, collected on a filter from the stack downstream of the gas-cleaning equipment, was provided for analysis.

The carbon content was determined using a Leco Model 521 apparatus. Samples of a standard ash were used to verify reproducibility with the low sample mass available for the submicron particles. Bulk ash density was determined by weighing 1-mL volumes.

A Cambridge Instruments S240 scanning electron microscope (SEM) and a JEOL 2000 FXII transmission electron microscope (TEM) were used to study particle morphology. The methods used to obtain well-dispersed particles for SEM examination included alcohol resuspension and filtering of bulk deposits, and short-duration (approximately 1 s) collection. Short-duration collection consisted of mounting a double-sided tape directly on the cascade impactor collection surfaces. Flow was established using dilution nitrogen, then the dilution flow was shut off for 1 s allowing combustion gas to enter the probe. This provided a partial layer of particles for imaging without any transfers that could transform particle morphology.

The power plant filter deposit was examined by both SEM and TEM using an alcohol suspension. The TEM was equipped with a Link AN10000 windowless energy-dispersive X-ray spectroscopy (EDS) detector that was used to examine the elemental composition of submicron particles. The EDS signals were corrected for the substrate background.

Results

Figure 1 shows the measured NO_x and the target stoichiometry along the length of the furnace. In the staged combustion and reburning cases, the main NO_x reduction occurs in the fuel-rich zones. Although the gas-stabilized, axial flame is nominally fuel lean, the design produces a very fuel-rich core near the burner. The most dramatic decrease (947 to 171 ppm NO_x) was achieved by creating an extremely long (1.5 s) fuel-rich zone.

The correlation between exit NO_x and carbon in the fly ash from Utah bituminous coal is shown in Fig. 2. The general trend of increasing carbon with decreasing NO_x is similar to previously reported results [3] for staged combustion. A limited number of experiments have been conducted with other fuels. The data for Illinois #6 bituminous coal are similar to the results reported for Utah coal. The carbon burnout was much higher for North Dakota lignite. Carbon ranged from about 1% for BASE to 6% for STG@1.5S conditions with slightly lower levels of NO_x than observed for Utah coal.

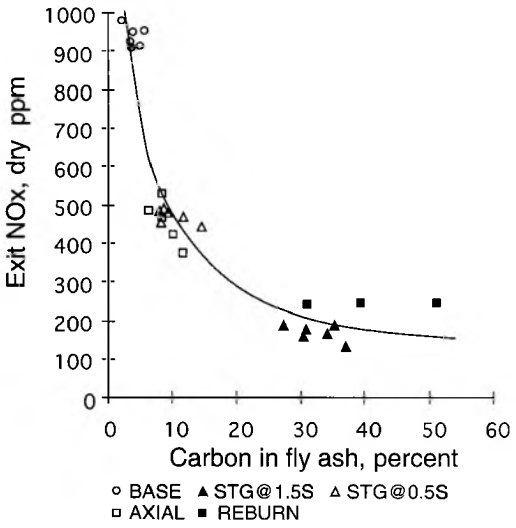

FIG. 2. Carbon in the total filter sample versus NO_x in the exit gas averaged over the particle sampling period. For the coal used in this study, 100 ppm NO_x equals approximately 0.064 g NO_2/MJ (0.15 lb NO_2/million BTU).

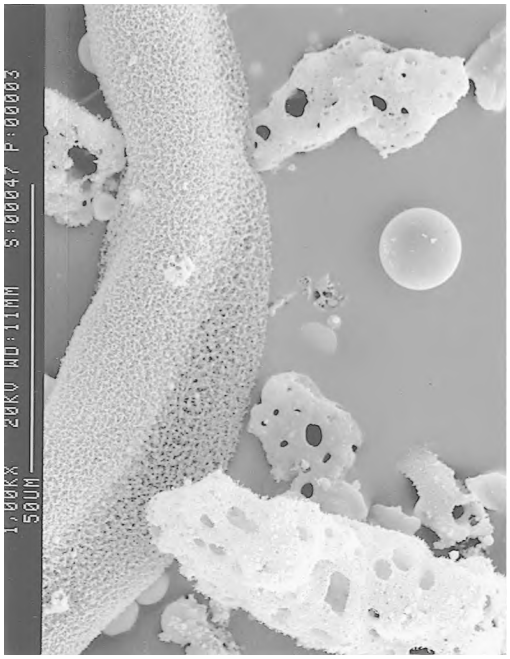

FIG. 3. SEM image (1000 X) of the cascade impactor preseparator material under condition STG@1.5S. Dense spheres, porous particles, and the large fine-grained structures are associated with mineral ash, partially burned char, and soot aggregates, respectively. The sample was obtained by short-duration collection 0.3 s downstream of the burnout air injection.

Electron microscopy showed that the fly ash contained three distinct types of particles: spheres, irregular porous particles, and aggregates of submicron primary particles, which were suspected to be mineral ash, unburned char, and soot. The smooth, dense spheres with a 1–10-μm diameter in pulverized coal fly ash are associated with melting and coagulation of minerals, whereas the submicron spheres are associated with mineral vaporization, nucleation, and coagulation [19]. Pulverized coal particles are transformed into porous, irregular char by devolatilization and heterogeneous partial oxidation [13]. Primary particles of soot, typically 10–100 nm diameter, can coagulate to form macroscopic aggregates.

The low-carbon ash samples from conditions BASE and AXIAL consisted almost entirely of spherical particles. The sample from condition STG@1.5S (Fig. 3) contained many large, fine-grained particles, up to 500 μm long by 25 μm wide, mixed with porous particles and spheres. The fly ash from condition STG@0.5S was intermediate between that of BASE and STG@1.5S. The fly ash from condition REBURN was a mixture of large porous particles and spherical particles with few fine-grained aggregates. Higher magnification showed that the fine-grained structures were formed from spherical particles smaller than 0.1 μm diameter. When the fly ash from condition STG@1.5S was resuspended in ethanol and filtered, the large fine-grained structures disappeared, the suspension turned opaque, and the filter was coated with a dense layer of submicron spheres.

The ethanol-resuspended sample from the power plant stack contained smooth spheres of mineral ash and aggregates of submicron spheres (see Fig. 4) but no porous particles resembling unburned char. The TEM showed that the clusters of primary particles from both condition STG@1.5S and the power plant had a morphology similiar to that reported for soot. The primary particle diameters were in the range of 20–50 nm.

The two reported mechanisms that produce agglomerates of submicron spheres from coal combustion are vaporization and condensation of metals, and soot formation [19]. Particle composition measurements by EDS using the SEM showed that the large spheres were composed of aluminum, silicon, and oxygen with lower levels of iron, calcium, and other metals. The fine-grained aggregate structures contained very low levels of crustal elements and trace metals. The porous particles from both conditions STG@1.5S and REBURN are intermediate in composition between the spheres and the fine-grained aggregates. This is consistent with the porous structures being unburned char with mineral inclusions still dispersed in the carbon matrix.

The TEM was used to obtain EDS spectra, including the low energy X-rays from carbon, from

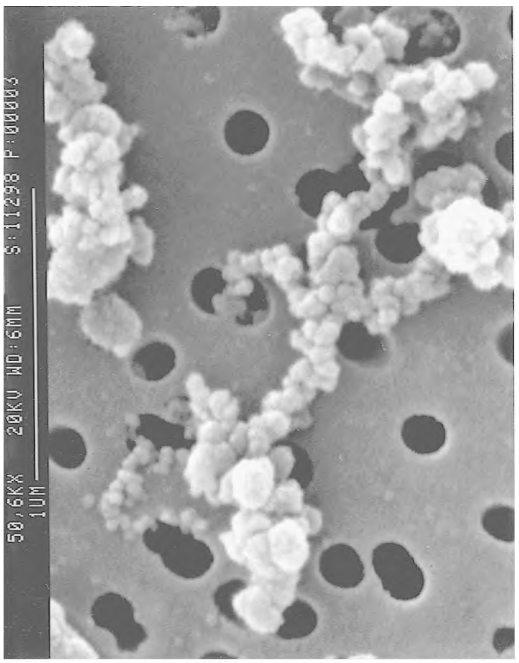

FIG. 4. SEM image (5100 X) of the black deposit collected on a filter from the stack of a power plant burning bituminous coal in a low-NO_x burner with over fire air. There were no particles with the characteristic morphology of coal char. EDS examination of the clusters of fine particles showed carbon, silicon, and oxygen with background levels of metals.

both dense submicron spheres and from the clusters of ultrafine spheres. The clusters of ultrafine spheres in the power plant sample contained carbon, oxygen, and silicon while the dense submicron spheres contained high levels of crustal elements. The laboratory-generated sample was similar, but little silicon was found mixed with the carbon.

The material deposited on various impactor stages by short-duration collection was examined by SEM. The preseparator, stage 0, and stage 1 samples ($d >$ 5.8-μm aerodynamic diameter) contained large soot aggregates, porous char particles, and mineral ash spheres. The samples from stages 3 and 5 (1.1–4.7-μm aerodynamic diameter) contained mostly spheres with some small soot aggregates and relatively few char particles. The stage 7 sample (0.43–0.65-μm aerodynamic diameter) contained submicron spheres mixed with 1–2-μm clusters of ultrafine particles.

The particle morphology observed by SEM and TEM supports the conclusion that the fly ash samples contain both soot and unburned char with the ratio of carbon forms varying with combustion conditions and particle size. The absence of significant levels of crustal elements and metals and the detection of carbon in the ultrafine particles do not support the alternative hypothesis that the aggregates of submicron particles in the high-carbon samples were formed by metal vaporization and condensation.

The mass of carbon per volume of furnace gas in the combined probe wash and total filter sample was highest close to the burner and decreased toward the exit port. Table 2 shows the carbon mass per volume of gas versus location for conditions BASE, STG@0.5S, and STG@1.5S. For the BASE condition, carbon (char and soot) oxidation is essentially complete by the first sampling port used in this study, which is 0.3–0.4 s from the burner, while under staged combustion conditions, the particles collected 0.4 s from the burner had low bulk density and high carbon content. This is consistent with a previous study that showed char burnout was 79–86% complete at a port 0.5 m (0.2 s) closer to the burner [16]. Comparing the carbon loading upstream and downstream of the staging air injection port shows that carbon burnout was much more rapid at the higher temperature of the STG@0.5S location compared to STG@1.5S. Little carbon burnout was measured across the last 2 m of the furnace.

Exit port carbon versus size data, shown in Fig. 5,

TABLE 2
Mass of carbon per volume of gas

Condition	Distance from Burner/m	BASE	STG@0.5S	STG@1.5S
Upstream of first staging port (used for STG@0.5S)	1.06	0.5	4.7	
Downstream, 0.20 s from first staging port	1.97		1.5	
Upstream of second staging port (used for STG@1.5S)	2.89			5.2
Downstream 0.28 s from second staging port	3.73	0.1	0.6	3.5
Exit sampling port	6.15	0.1	0.3	2.3

Data are the average of two replicates expressed as grams of carbon per m^3. Concentrations are on a dry, 1 atm, 298 K basis and are corrected to 3% O_2 to remove the effect of dilution at the staging port.

100% of fuel carbon = 85 g/m^3, 100% of ASTM volatiles = 49 g/m^3.

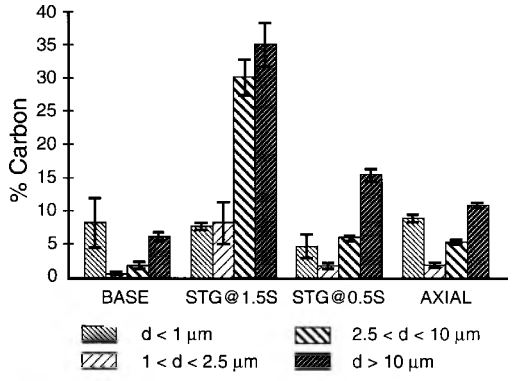

FIG. 5. Carbon content versus particle size range in exit port samples for the base case, axial burner, and two staged combustion conditions. Sampling at upstream ports showed a similar minimum carbon content in intermediate diameter particles. Data are the mean ± standard deviation.

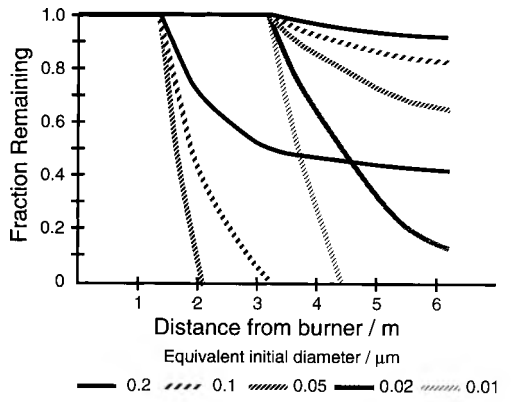

FIG. 6. Calculated carbon burnout using the Nagle and Strickland-Constable formula and the measured furnace temperature profile. Hypothetical soot aggregates of various initial sizes are characterized by the ratio of effective surface area to mass, expressed as an equivalent sphere (e.g., 60 $m^2/g \approx 0.05\ \mu m$ diameter). The starting locations at 1.3 and 3.1 m from the coal burner correspond to the STG@0.5S and STG@1.5S staging air locations, respectively. The calculations indicate that the temperature-dependent oxidation rate downstream of the reducing zone can account for the observed difference in exit carbon between conditions STG@0.5S and STG@1.5S.

indicates that the carbon-containing particles are bimodally distributed. For all conditions, the carbon content decreased with decreasing particle size down to the fraction between 1 and 2.5 μm. For all conditions except STG@1.5S, the carbon in the submicron particle fraction was higher than in the 1–2.5-μm fraction. The deposits collected in the impactor for all conditions showed a color trend from black or dark gray for the largest particles to light gray or brown for the middle sizes, then darker again on the final filter. The preseparator carbon ash from condition STG@1.5S had a bulk density of 0.097 ± 0.003 g/cc, which is significantly (>99% confidence factor) lower than either the 0.36 ± 0.02 g/cc density of fly ash from condition BASE or the 0.33 ± 0.02 g/cc density of char prepared from the same coal by extraction from near the flame and rapid quenching [16]. This decrease in bulk density is explained by the SEM observation of large numbers of soot aggregates in the ash from condition STG@1.5S.

The SEM images give no information on the relative amount of soot and char since the true densities of the porous and aggregate particles are unknown. A method to estimate the ratio of the soot and char by ultrasonic dispersal of the aggregates followed by differential settling is under development and is reported elsewhere [17]. Preliminary results are that, under the staged combustion conditions used in these experiments, 5–20% by weight of the fly ash is ultrafine soot particles. This indicates the soot may not be insignificant compared to unburned char under low-NO_x combustion conditions.

Kinetic Calculations

Kinetic calculations were made to determine whether a soot particle that began oxidizing at the staging air injection plane would be expected to survive to the furnace exit. Rates of mass loss per area (g carbon/cm^2 s) as a function of oxygen and temperature were obtained using the semiempirical formula for soot oxidation rate first proposed by Nagle and Strickland-Constable [20] and found in standard references [21].[1] It is recognized that the Nagle and Strickland-Constable correlation overstates soot oxidation at temperatures below 1800 K [22] and understates the oxidation rate at low-oxygen conditions [21] where OH radicals are important. These kinetic calculations, however, are for the purposes of explaining the observed trends rather than for fitting the data.

The curves for mass remaining versus position shown in Fig. 6 were obtained by numerically integrating the reaction rate at the measured furnace temperature assuming plug-flow velocity with burnout starting at the air injection locations used for conditions STG@0.5S and STG@1.5S. The particle diameter in the calculations was varied from a value representative of a primary soot particle (10 nm) to

[1]Fossil Fuel Combustion [21] incorrectly lists the sign of the exponent in the pre-exponential coefficient for K_T. The correct value is $1.15 \times 10^{+5}$.

a value of 0.2 μm to illustrate the impact of particle agglomeration. These equivalent diameters are interpreted as the size of a solid sphere that has the same effective surface area to volume ratio as the soot aggregate. A detailed oxidation model would need to allow for details of the aggregate pore structure and is outside the scope of this combustion emissions investigation. Because of the temperature gradients in the furnace, soot burnout greatly decreases when staging air is injected at 1.5 s rather than at 0.5 s. These calculations support the hypothesis that the difference in carbon content between conditions STG@1.5S and STG@0.5S reported in Table 2 is the result of the temperature-dependent soot burnout rate. In order to match the experimental data, one would need better measures of the relative mass of char and soot, of the soot aggregation, and of the kinetics pertinent to the coal char and soot in question.

Conclusions

This study showed that both soot and unburned char are present in the high-carbon fly ash collected at the furnace exit under low-NO_x pulverized bituminous coal combustion conditions. The formation of soot aggregates is consistent with previous studies of coal combustion in drop-tube furnaces. The incomplete burnout of soot aggregates between the end of the fuel-rich zone and the furnace exit indicates that there is insufficient time at elevated temperature to complete soot oxidation. The detection of soot aggregates in the high-carbon fly ash obtained from the stack of a power plant when operating low-NO_x burners indicates that soot in the fly ash is not an artifact of the laboratory furnace but can also be a problem in the field. At a time when unburned carbon from the introduction of low-NO_x burners has become a problem in power generation stations, the detection of soot aggregates that can persist for long times indicates that this source of carbon loss needs to be considered.

Acknowledgments

This work was supported in part by the U.S. Department of Energy University Coal Research Program Grant and U.S. Department of Energy PRDA. The assistance of Jacob Brouwer, Kevin Davis, and Stan Harding of Reaction Engineering International regarding full-scale combustion data is appreciated.

REFERENCES

1. Chen, S. L., Heap, M. P., Pershing, D. W., and Martin, G. B., "Influence of Coal Composition on the Fate of Volatile and Char Nitrogen during Combustion," in *Nineteenth Symposium (International) on Combustion*, The Combustion Institute, Pittsburgh, 1982, pp. 1271–1280.
2. Storm, R. F., *Power* 53–62 (1993).
3. Maier, H., Spliethoff, H., Kicherer, A., Fingerle, A., and Hein, K. R. G., *Fuel* 73:1447–1452 (1994).
4. Chuang, J. C., Wise, S. A., Cao, S., and Mumford, J. L., *Environ. Sci. Technol.* 26:999–1004 (1992).
5. Morris, W. A., Versteeg, J. K., Bryant, D. W., Legzdins, A. E., McCarry, B. E., and Marvin, C. H., *Atmospheric Environ.* 29:3441–3450 (1995).
6. Mumford, J. L., Helmes, C. T., Lee, X., Seidenberg, J., and Nesnow, S., *Carcinogenesis* 11:397–404 (1990).
7. Mitra, A., Sarofim, A. F., and Bar-Ziv, E., *Aerosol Sci. Technol.* 6:261–271 (1987).
8. Fletcher, T. H., Ma, J., Rigby, J. R., Brown, A. L., and Webb, B. W., *Prog. Energy Combust. Sci.* 23:283–301 (1997).
9. Chen, J. C. and Niksa, S., "Suppressed Nitrogen Evolution from Coal-Derived Soot and Low-Volatility Coal Chars," in *Twenty-Fourth Symposium (International) on Combustion*, The Combustion Institute, Pittsburgh, 1992, pp. 1269–1276.
10. Hurt, R. H. and Davis, K. A., "Near-Extinction and Final Burnout in Coal Combustion," in *Twenty-Fifth Symposium (International) on Combustion*, The Combustion Institute, Pittsburgh, 1994, pp. 561–568.
11. Walsh, P. M., Xie, J., Douglas, R. E., Battista, J. J., and Zawadzki, E. A., *Fuel* 73:1074–1081 (1994).
12. Shibaoka, M., *Fuel* 65:449–450 (1986).
13. Unsworth, J. F., Barratt, D. J., and Roberts, P. T., *Coal Quality and Combustion Performance*, Elsevier, Amsterdam, 1991.
14. Seeker, W. R., Samuelsen, G. S., Heap, M. P., and Trolinger, J. D., "The Thermal Decomposition of Pulverized Coal Particles," in *Eighteenth Symposium (International) on Combustion*, The Combustion Institute, Pittsburgh, 1981, pp. 1213–1226.
15. McLean, W. J., Hardesty, D. R., and Pohl, J. H., "Direct Observations of Devolatilizing Pulverized Coal Particles in a Combustion Environment," in *Eighteenth Symposium (International) on Combustion*, The Combustion Institute, Pittsburgh, 1981, pp. 1239–1248.
16. Spinti, J. C. P., Ph.D. dissertation, University of Utah, 1997.
17. Veranth, J. M., Ph.D. dissertation, University of Utah, 1998.
18. Smith, K. R. and Aust, A. E., *Chem. Res. Toxicol.*, in press.
19. Flagan, R. C. and Seinfeld, J. H., *Fundamentals of Air Pollution Engineering*, Prentice Hall, Englewood Cliffs, NJ, 1988.
20. Park, C. and Appleton, J. P., *Combust. Flame* 20:369–379 (1973).
21. Haynes, B. S., in *Fossil Fuel Combustion* (A. F. Sarofim and W. Bartok, eds.), Wiley Interscience, New York, 1991.
22. Kennedy, I. M., *Prog. Energy Combust. Sci.* 23:95–132 (1997).

COMMENTS

Arun Mehta, EPRI, USA.

1. Where in the boiler was the probe located—waterwell with SH/RH?
2. Did you simulate the gas velocity in a real boiler in order to simulate ash particle impaction behavior?
3. Did you see many soot particles on the flyash particle (5–10 μm) surfaces?

Author's Reply. The sample location used for collecting the samples reported in this paper corresponds roughly to the residence time and gas temperature conditions in the economizer of a real boiler. The laboratory furnace was designed to simulate the gas residence time of a full-scale boiler, so the velocities had to be much lower than in a utility boiler to allow a reasonable furnace length.

Some ultrafine particles were observed on the surface of larger particles in the samples generated by short-duration collection, but Fig. 3 is typical of the archived images. Other SEM samples were prepared by alcohol suspension of the particles followed by dilution and filtering onto a polycarbonate membrane. In these images, it is impossible to determine whether the ultrafines found on the surface of larger particles were deposited while in the furnace or are an artifact of the sample procedure.

•

Roman Weber, International Flame Research Foundation, The Netherlands. Is your U-shaped reactor suitable for the experiments you have carried out? Do you know what happens in the corners of the reactor and in its horizontal section? Perhaps there is a substantial deposition of particles on the walls. Perhaps the largest particles grow on the walls and later are picked up by the flow. I would suggest repeating the experiment in a vertical plug-flow reactor.

Author's Reply. The furnace was designed for studies on NO_x formation and control (see previous comment) but has since been adapted for particle pollutant studies. Large particles are deposited in an ash bin located in the furnace corner directly below the burner. Ash also settles along the horizontal section of the furnace and is periodically removed. Typical partitioning between bottom ash and fly ash in a dry bottom utility boiler is about 20% bottom ash while the fraction deposited in the U-furnace is over half. Based on the transient change observed in exit oxygen after switching between coal and the overnight natural gas flame, we know that a substantial amount of carbonaceous material is deposited in the furnace during staged pulverized coal combustion experiments.

The suggestion to rerun the experiments in vertical furnace is appreciated. We plan to conduct similar experiments in a 400-kW straight, horizontal furnace with a 1-m-square cross section. This will test whether the observed large soot aggregates are an artifact of the small diameter and low Reynolds number of the U-furnace.